

Detection of quantum phases via out-of-time-order correlators

Ceren B. Dağ* and Kai Sun

Department of Physics, University of Michigan, Ann Arbor, Michigan 48109, USA

L.-M. Duan

Center for Quantum Information, IIIS, Tsinghua University, Beijing 100084, PR China.

(Dated: November 29, 2022)

We elucidate the relation between out-of-time-order correlators (OTOCs) and the phase transitions via analytically studying the OTOC dynamics in degenerate spectrum. Our method points to key ingredients to dynamically detect quantum phases as well as their symmetry breaking patterns via out-of-time-order correlators for a wide range of quantum phase transitions. We apply our method to a critical model, XXZ model that numerically confirms our predictions.

Out-of-time-order correlators (OTOCs) [1] probe information scrambling in quantum systems of different nature [2–6] and reflect the symmetries [7] or lack thereof [8, 9] of the underlying Hamiltonian. It has been recently observed that the OTOC is also susceptible to phase transitions [10]. Specifically, the saturation value of OTOC seems to be an indicator of the ordered or disordered phase in (non-)integrable Ising Model with transverse field in equilibrium and dynamical phase transitions [10].

In this paper, we develop a method on OTOC dynamics to obtain intuition for the emerging relation between quantum phase transitions and out-of-time-order correlators. We find that the OTOC saturation value could detect the degeneracy in ground-state(s) and the ground state physics is the leading order contribution to the OTOC, under the criteria that our method provides. Therefore, we reach to the conclusion that the OTOC is susceptible to long-range order, while the quasi-long range order is not visible to it. To verify our method, we study the dynamics of 1D critical XXZ chain, where there are Ising and critical XY phases.

Method. Our aim is to be able to come up with an expression that predicts the saturation value of OTOC for long times in the spirit of Eigenstate Thermalization Hypothesis (ETH) [11, 12]. The out-of-time-order correlation function can be defined as

$$F(t) = \langle W^\dagger(t) V^\dagger W(t) V \rangle, \quad (1)$$

where V and W are local operators and the expectation value is over an initial state $|\psi(0)\rangle$. This initial state could be chosen as the ground state [6, 10], or a random state drawn from Haar measure [13] to imitate $\beta = 0$ temperature state [14]. Eventually, the original definition that is the commutator growth $-\text{Tr} \left(\frac{\exp[-\beta H]}{Z} [W(t), V]^2 \right)$ [9] could be re-expressed in terms of the OTOC of operators W and V with an initial state at the inverse temperature β . Therefore we can probe the information scrambling through OTOCs [6, 15, 16].

Given $|\psi(t)\rangle = \sum_\alpha c_\alpha e^{-iE_\alpha t} |\psi_\alpha\rangle$, where $|\psi_\alpha\rangle$ are eigenstates of the Hamiltonian with the associated eigen-

values E_α , we define a modified initial state $|\psi'(0)\rangle = V |\psi(0)\rangle$ and have $|\psi'(t)\rangle = \sum_\beta b_\beta e^{-iE_\beta t} |\psi_\beta\rangle$. Then the OTOC, Eq. (1), can be recast to a fidelity measure of 3-point function,

$$F(t) = \langle \psi(t) | W^\dagger e^{-iHt} V^\dagger e^{iHt} W | \psi'(t) \rangle, \\ = \sum_{\alpha, \beta} c_\alpha^* b_\beta e^{-i(E_\beta - E_\alpha)t} \langle \psi_\alpha | W^\dagger V^\dagger(t) W | \psi_\beta \rangle. \quad (2)$$

The expectation value $\langle \psi_\alpha | W^\dagger V^\dagger(t) W | \psi_\beta \rangle$ in Eq. (2) can be written as

$$\sum_{\gamma, \gamma'} e^{-i(E_\gamma - E_{\gamma'})t} \langle \psi_\alpha | W^\dagger | \psi_\gamma \rangle \langle \psi_\gamma | V^\dagger | \psi_{\gamma'} \rangle \langle \psi_{\gamma'} | W | \psi_\beta \rangle,$$

with the help of completeness relation $\sum_\gamma |\psi_\gamma\rangle \langle \psi_\gamma| = \mathbb{I}$. Then the OTOC becomes,

$$F(t) = \sum_{\alpha, \beta, \gamma, \gamma'} c_\alpha^* b_\beta e^{-i(E_\beta - E_\alpha + E_\gamma - E_{\gamma'})t} W_{\alpha\gamma}^\dagger V_{\gamma\gamma'}^\dagger W_{\gamma'\beta},$$

where $\langle \psi_\alpha | W | \psi_\gamma \rangle = W_{\alpha\gamma}$ are EEVs (eigenstate expectation values) [17]. Now one can derive the saturation value for long times as well as dynamical features, such as revival timescales in integrable Hamiltonians based on the technique in Ref. [18].

Let us study the saturation value in long times, since this value is expected to contain the signature of quantum phases. For long enough times, equilibration in OTOC dynamics can be obtained only when the phase decoheres. Then the equilibration value can be obtained by requesting $E_\beta - E_\alpha + E_\gamma - E_{\gamma'} = 0$. This condition can be satisfied with four different scenarios: (i) $E_\alpha = E_\beta$ and $E_\gamma = E_{\gamma'}$; (ii) $E_\alpha = E_\gamma$ and $E_\beta = E_{\gamma'}$; (iii) $E_\alpha = E_\beta = E_\gamma = E_{\gamma'}$, which is contained both in (i) and (ii); (iv) $E_\beta - E_\alpha + E_\gamma - E_{\gamma'} = 0$ with $E_\beta \neq E_\alpha \neq E_\gamma \neq E_{\gamma'}$. If a non-degenerate spectrum is assumed, i.e. $E_\alpha = E_\beta$ implies $\alpha = \beta$, the OTOC reduces to,

$$F_{t \rightarrow \infty} = \sum_{\alpha, \gamma} c_\alpha^* b_\alpha |W_{\alpha\gamma}|^2 V_{\gamma\gamma}^\dagger + \sum_{\alpha, \beta} c_\alpha^* b_\beta W_{\alpha\alpha}^\dagger V_{\alpha\beta}^\dagger W_{\beta\beta} \quad (3) \\ - \sum_{\alpha} c_\alpha^* b_\alpha |W_{\alpha\alpha}|^2 V_{\alpha\alpha}^\dagger + \sum_{\alpha \neq \beta \neq \gamma \neq \gamma'} c_\alpha^* b_\beta W_{\alpha\gamma}^\dagger V_{\gamma\gamma'}^\dagger W_{\gamma'\beta},$$

with four terms corresponding to four conditions (i)-(iv), respectively. Eq. (3) straightforwardly shows why quantum chaotic spin systems should eventually decay to zero when ETH is evoked. However we leave this discussion to elsewhere since it deviates from the central focus of this work. For the study of quantum phase transition and quantum criticality, Eq. (3) is not sufficient due to its non-degenerate assumption, because a quantum phase transition usually involves energy degeneracy, e.g. degeneracy from spontaneous symmetry breaking or topological degeneracy from topological order. Thus, we need to generalize Eq. (3) to a more generic form, which allows degeneracy in the energy spectra. We group all eigenstates of the Hamiltonian into degenerate sets labeled by θ , and each state in its corresponding set is denoted by α for an eigenstate $\psi_{[\theta,\alpha]}$. The OTOC can be reorganized with the new notation, which is one main result of this Letter,

$$F(t \rightarrow \infty) = \sum_{\theta\theta'} \sum_{\alpha\beta\gamma\gamma'} c_{[\theta,\alpha]}^* \left(b_{[\theta,\beta]} W_{[\theta,\alpha][\theta',\gamma]}^\dagger V_{[\theta',\gamma][\theta',\gamma']}^\dagger W_{[\theta',\gamma'][\theta,\beta]} + b_{[\theta',\beta]} W_{[\theta,\alpha][\theta,\gamma]}^\dagger V_{[\theta,\gamma][\theta',\gamma']}^\dagger W_{[\theta',\gamma'][\theta',\beta]} \right) \quad (4)$$

$$+ \sum_{\alpha\beta\gamma\gamma'} \left(- \sum_{\theta} c_{[\theta,\alpha]}^* b_{[\theta,\beta]} W_{[\theta,\alpha][\theta,\gamma]}^\dagger V_{[\theta,\gamma][\theta,\gamma']}^\dagger W_{[\theta,\gamma'][\theta,\beta]} + \sum_{\theta \neq \theta' \neq \phi \neq \phi'} c_{[\theta,\alpha]}^* b_{[\theta',\beta]} W_{[\theta,\alpha][\phi,\gamma]}^\dagger V_{[\phi,\gamma][\phi',\gamma']}^\dagger W_{[\phi',\gamma'][\theta',\beta]} \right).$$

Here, $\theta, \theta', \phi, \phi'$ denote degenerate sets while $\alpha, \beta, \gamma, \gamma'$ denote quantum states in their corresponding sets. Eq. (4) is the generalization of Eq. (3) for a spectrum with degenerate subspaces and predicts the saturation value of OTOC accurately if the OTOC saturates. If the OTOC does not saturate, Eq. (4) still accurately predicts the time-average of sufficiently long-time dynamics.

We look for the criteria of that the ground state subspace contribution is the leading order in the OTOC saturation value Eq. (4). For this, we first choose $W = V$ as the order parameter operator and expand the coefficients $b_{[\theta,\beta]} = \sum_{\kappa,\tau} W_{[\theta,\beta][\kappa,\tau]} c_{[\kappa,\tau]}$ in Eq. (4) for the clarity of the argument. If (i) the initial state is set to the state where the phase transition is expected to happen, e.g. the ground state(s) $c_{[1,1]} = 1$; and (ii) we apply an ansatz on the matrix elements of the operator projected on this state, e.g. $|W_{[1,\alpha][\theta,\beta]}| \ll 1$, where $\theta \neq 1$ is a different energy subspace than the subspace of the ground state(s), we observe the following dynamical decomposition:

$$F(t \rightarrow \infty) = F_{\text{gs}}(t \rightarrow \infty) + F_{\text{ex}}(t \rightarrow \infty). \quad (5)$$

Here $F_{\text{gs}}(t \rightarrow \infty)$ is the ground subspace contribution, whereas the $F_{\text{ex}}(t \rightarrow \infty)$ is the contribution of higher energy excitations. The latter is a correction to the ground-state physics in the OTOC saturation value, when the criteria are satisfied. The assumption on the initial state sets the scrambling discussed in the rest of the paper to effectively zero temperature. Whereas the operator ansatz becomes even more specific for the phase of interest. If there is a symmetry-broken long-range order to capture, the fluctuations between the matrix elements of the operator are suppressed in the ground state subspace, meaning there is at least a pair of matrix elements accumulating the order $\rightarrow |W_{[1,\alpha][1,\beta]}| \sim \mathcal{O}(1)$. This modifies the operator ansatz as $|W_{[1,\alpha][1,\beta]}| \gg |W_{[1,\gamma][\theta,\gamma']}|$ for the ordered phase. Thus, we derive the expression for

eracy from spontaneous symmetry breaking or topological degeneracy from topological order. Thus, we need to generalize Eq. (3) to a more generic form, which allows degeneracy in the energy spectra. We group all eigenstates of the Hamiltonian into degenerate sets labeled by θ , and each state in its corresponding set is denoted by α for an eigenstate $\psi_{[\theta,\alpha]}$. The OTOC can be reorganized with the new notation, which is one main result of this Letter,

$F_{\text{gs}}(t \rightarrow \infty)$ in the ordered phase as,

$$F_{\text{gs}}(t \rightarrow \infty) \sim \sum_{\beta,\gamma,\gamma'} W_{[1,1][1,\gamma]} W_{[1,\gamma][1,\gamma']} W_{[1,\gamma'][1,\beta]} W_{[1,\beta][1,1]}, \quad (6)$$

while the operator ansatz simultaneously implies that the OTOC is dominated by the ground state physics, $F_{\text{gs}} \gg F_{\text{ex}}$ in the ordered phase. On the other hand, the fluctuations between the matrix elements of the operator are maximal in a disordered phase, implying $W_{[1,\alpha][1,\beta]} \sim 0$ for all in the ground state subspace which results in $F_{\text{gs}}(t \rightarrow \infty) \sim 0$. Therefore, the OTOC is dominated by the correction terms that are contributed by the excitations in the spectrum $F_{\text{ex}}(t \rightarrow \infty)$. However, the operator ansatz $|W_{[1,\alpha][\theta,\beta]}| \ll 1$ guarantees a bounded correction term $F_{\text{ex}}(t \rightarrow \infty) \ll 1$. As a result, (i) the OTOC is able to capture the degeneracy in the ground state (Eq. (6)) and, (ii) the correction of the excited states always remains bounded; all of which explains why the OTOC differentiates an ordered phase from a disordered one, e.g. in ground state [10] or excited-state [19] phase transitions. A mixed initial state (e.g. finite or infinite temperature) violates our initial state assumption, hence suggesting a smoothed phase boundary by washing away the sharp signature at the transition point [20].

Eq. (6) provides us a low-cost alternative to simulating the real-time dynamics in the computation of the OTOC saturation value when we use the OTOC to probe the criticality: Lanczos diagonalization to determine only the ground states could replace the exact diagonalization of dynamics computation to give the leading order term in the symmetry-broken order. Further, Eq. (6) clearly exhibits how the OTOC can suffer from the finite-size effects. Imagine that the finite-size lifts the degeneracy; then we would write the ground state contribution to the OTOC as

$$|W_{[1,1][1,2]} W_{[1,2][1,1]}|^2 \exp[-2i(E_{[1,2]} - E_{[1,1]})t]. \quad (7)$$

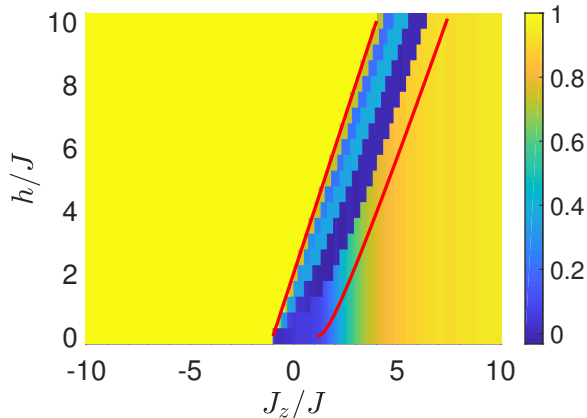


FIG. 1. Phase diagram based on the OTOC saturation values via Eq. (4), x-axis is the spin interaction strength in the z -direction J_z and y-axis is the magnetic field h , for $N = 13$ system size and σ_z^i bulk spin operator, when open boundary conditions are set and the initial state is a ground state. The red lines are the phase boundaries based on Bethe ansatz technique for infinite-size system [21].

Since Eq. (7) is the dominant contribution to the OTOC in the ordered phase, the order will eventually be invisible to the saturation value, and it will be encoded in the frequency spectrum of the OTOC. This encourages us to state that the relation between the zero-temperature scrambling and the phase transitions could be seen as an effect of ‘pre-scrambling’, when the size is finite. The period of the emerging oscillation (due to degeneracy-lifting) is $\tau = \pi/(E_{[1,2]} - E_{[1,1]})$. Then starting from $t \sim \tau/2$, the order will be invisible to the saturation value. Thus, the pre-scrambling region, the region where the system seems to have reached its most correlated state, could be defined for $t \ll \tau/2$; whereas the order will be most visible to the frequency spectrum around $t \gg \tau/2$. Further, the ground state contribution will exist in the saturation value as a non-zero effect for a time $t \sim \tau/4$, where the time-averaging will reveal the order. The relation between time and energy spectrum reflects how better we resolve the energy spectrum with a longer time evolution. This, in turn, helps us to estimate the time interval of the corresponding dynamics simulation of the theory Eq. (4), even though Eq. (4) is explicitly time-independent.

Finally, we predict that the ground state contribution to the OTOC saturation cannot efficiently distinguish quasi-long range order from a disordered phase. Because, the quasi-long range order produces zero expectation value for the order parameter (per site): $W_{[1,\alpha][1,\beta]} \sim 0$, similar to a disordered phase, and hence $F_{\text{gs}}(t \rightarrow \infty) \sim 0$ follows with correction term dominating the OTOC saturation $F(t \rightarrow \infty)$. Next we are going to test this idea as well as our theory on the 1D XXZ-model.

Model and results. The Hamiltonian of XXZ-Model

reads,

$$H = J \sum_i \left(\sigma_i^x \sigma_{i+1}^x + \sigma_i^y \sigma_{i+1}^y + \frac{J_z}{J} \sigma_i^z \sigma_{i+1}^z \right) + h \sum_i \sigma_i^z,$$

where σ_i^n are spin-1/2 Pauli matrices with energy scale set to J and hence time scale set to $1/J$; J_z/J and h are the z -axis spin coupling strength and the magnetic field strength, respectively. The red lines in Fig. 1 show the phase boundaries produced by an exact method (Bethe Ansatz) for an infinite-size system. Therefore, this model has three phases: two gapped Ising phases (ferromagnetic and antiferromagnetic) at large $|J_z/J|$ and a gapless XY phase with quasi-long range order for small $|J_z/J|$, i.e. the Berezinskii-Kosterlitz-Thouless transition [22, 23]. We choose the OTOC operators as σ_i^z or σ_i^x for the spin at the i th site, based on the order parameters of the ferromagnetic Ising phase ($\sum_i \sigma_i^z$), antiferromagnetic Ising phase ($\sum_i (-1)^i \sigma_i^z$), and the XY-phase ($\sum_i \sigma_i^x$). Fig. 1 shows the phase diagram based on the saturation values of OTOCs with σ_i^z [computed using Eq. (4) for a system of $N = 13$ spins]. We numerically confirm our theory with OTOC saturation values that are either nonzero or nearly zero in the Ising and XY phases. In fact, the OTOC recovers the phase boundaries of the Bethe ansatz solution: the agreement is perfect at the ferromagnetic-XY phase boundary and approximate at the antiferromagnetic-XY boundary due to finite-size effects [24]. Let us detail the physics in the following discussion.

We plot two cross-sections from Fig. 1 in Fig. 2a where the lines with orange-squares ($h = 0$) and blue-circles ($h = 4$ [J]) are the saturation values, Eq. (4) for time $\Delta t \sim \frac{\pi}{4} 10^3$ [1/J] (via energy-time relation). We also plot the leading order term in the saturation, $F_{\text{gs}}(t \rightarrow \infty)$ in Fig. 2a with purple-cross ($h = 0$) and red-diamond ($h = 4$) lines. The OTOC saturation exactly reduces to the ground state contribution with no correction $F_{\text{ex}} = 0$ in the Ising-ferromagnet, meaning that the saturation value in the ordered phase is exactly predicted by the Eq. (6). The reason follows as: the spins are fully polarized in the ferromagnetic ground states, and they belong to the opposite magnetization sectors of the Hamiltonian which has magnetization conservation $[H, S_z] = 0$ ($S_z = \sum_i \sigma_i^z$). Since they are the only states of their corresponding magnetization sectors, the fluctuations in the matrix elements are exactly zero, $|W_{[1,\alpha][\theta,\beta]}| = 0$. This is why the system does not scramble at all $F(t \rightarrow \infty) = 1$, even though the XXZ-model is an interacting model. We emphasize that this non-scrambling is not due to integrability of XXZ model, rather it is the signature of critical order. The rotational symmetry also protects the ferromagnetic ground states from hybridizing, all of which results in no finite-size effects at the phase boundary from ferromagnet to XY-paramagnet. In the disordered-XY phase ($h = 0$), the ground state contribution is zero $F_{\text{gs}} = 0$, leaving the correction term to dominate the

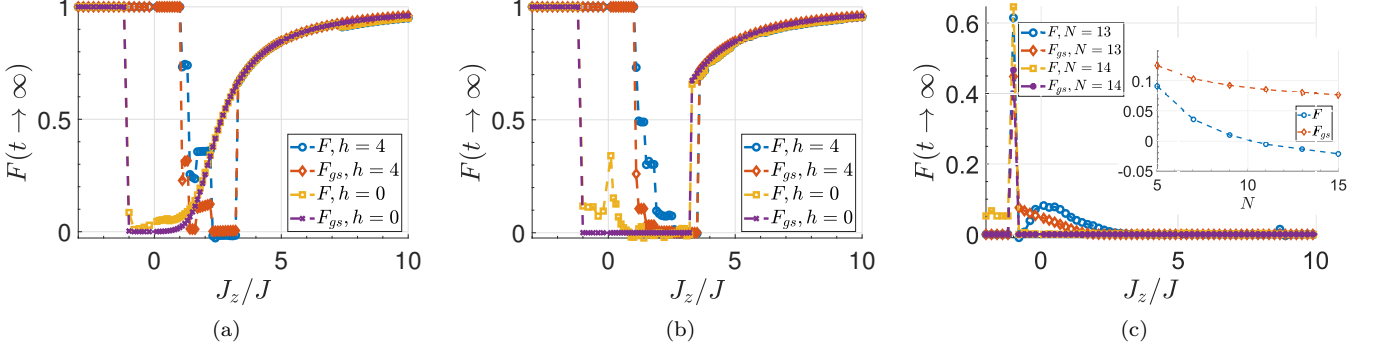


FIG. 2. The OTOC saturation values for (a) an open-boundary chain with $N = 13$ size and time of $\frac{\pi}{4}10^3 [1/J]$ and (b) a periodic-boundary chain with $N = 14$ size and time of $\frac{\pi}{4}10 [1/J]$ at fields $h = 0$ (orange-squares: Eq. (4), purple-crosses: Eq. (6)) and $h = 4$ [J] (blue-circles: Eq. (4), red-diamonds: Eq. (6)), for σ_i^z operator. (c) The OTOC saturation values for σ_i^x operator at $h = 0$, $N = 13$ (blue-circles: Eq. (4), red-diamonds: Eq. (6)) and $N = 14$ (orange-squares: Eq. (4), purple-crosses: Eq. (6)) for time $\frac{\pi}{4}10^3 [1/J]$. Inset: System-size scaling of Eq. (4) (blue-circles) and Eq. (6) (red-diamonds) at $J_z/J = -0.9$.

saturation value, however with a small magnitude as explained above. This is the reason of mismatch between the OTOC saturation value and its leading order term, seen in the XY-phase of Figs. 2a-2b, while we are still able to differentiate the disordered phase from the ordered phases. Finally, in the Ising-antiferromagnet the exact agreement between Eqs. (4) and (6) takes place only at the $J_z/J \rightarrow \infty$ limit. As we approach the phase boundary to XY-phase, the fluctuations between matrix elements gradually increase, $|W_{[1,\alpha][1,\beta]}| \rightarrow 0$, result in a nonzero but small correction term to the ground-state contribution and eventually drive the phase transition. For a phase transition that involves antiferromagnetic order, due to the doubling of the unit cell size, it is not uncommon that the finite-size contributions may oscillate as we increase the system size, depending on whether the system is composed of even (Fig. 2b) or odd (Fig. 2a) number of sites. For periodic boundary conditions, the systems with even number of sites usually show smaller finite-size effects. In our studies, though, we observe the opposite: chains with odd number of spins experience finite-size effects less. We explain why in the following: As far as the OTOC is concerned, stronger finite size effects are expected for systems with even number of sites, since the key to obtain the OTOC saturation value is to sum over all the quantum states in the ground state subspace. In an Ising-ordered phase, an exact two-fold degeneracy is guaranteed for a chain with odd number of spins by the Kramers degeneracy theorem, because an odd number of spin-1/2 results in a half-integer total spin. For a system with even number of sites (i.e. integer total spin), such an exact degeneracy is not expected and thus the degeneracy is lifted by finite size effects more strongly than chains with odd number of spins. This explains the dramatic difference between Figs. 2a-2b at the XY-antiferromagnet boundary. We also note that the

ground states belong to the $S_z = 0$ magnetization sector in the antiferromagnet, which is the biggest sector of the Hamiltonian and hence they would hybridize with each other.

We plot the OTOC with σ_i^x operator for $N = 13$ (blue-circles) in Fig. 2c: the OTOC saturation remains small in all three phases and thus the OTOC can hardly distinguish the XY-ordered from XY-disordered phases. When the chains with even number of spins are used ($N = 14$, orange-squares) in the theory, we do not even obtain any difference between the phases. This is in agreement with our theoretical predictions discussed previously. Additionally, the fluctuations between the matrix elements of quasi-long range order parameter σ_i^x are always maximal regardless of the phase. Hence, we observe the mismatch between the OTOC saturation and its ground state contribution (red-diamonds $N = 13$ and purple crosses $N = 14$). The inset of Fig. 2c shows that the OTOC saturation value and its ground state contribution, both, decrease with the system size for odd-numbered chains, exhibiting that the OTOC saturation cannot capture the quasi-long range order in bigger systems and thermodynamic limit. We briefly note that the detection of the order at $J_z/J = -1$ is robust due to the massive degeneracy in the ground state at this point of different symmetry (SU(2) symmetry).

Conclusion. Our theoretical predictions on XXZ model can be experimented with cold atoms [25]. Based on the studies in literature [10, 19, 20] and our results in XXZ-model, our method seems to be universal in explaining the reasoning behind the relation between scrambling and the quantum criticality. In this sense, our method is an analogue of Eigenstate Thermalization Hypothesis: It tells us the criteria of how scrambling probes the criticality; though it is independent of the integrability of the system, unlike ETH. We conclude, given that the initial

state is a ground state, the OTOC could be used to dynamically detect the quantum phases with long-range order and capture the symmetry-breaking quantum phase transitions.

Acknowledgements. C.B.D. thanks P. Myles Eugenio for interesting discussions and comments on the manuscript.

[24] See supplementary material.

[25] L.-M. Duan, E. Demler, and M. D. Lukin, Phys. Rev. Lett. **91**, 090402 (2003).

* cbdag@umich.edu

- [1] A. I. Larkin and Y. N. Ovchinnikov, Soviet Journal of Experimental and Theoretical Physics **28**, 1200 (1969).
- [2] Y. Sekino and L. Susskind, Journal of High Energy Physics **10**, 065 (2008), arXiv:0808.2096 [hep-th].
- [3] N. Lashkari, D. Stanford, M. Hastings, T. Osborne, and P. Hayden, Journal of High Energy Physics **4**, 22 (2013), arXiv:1111.6580 [hep-th].
- [4] B. Swingle and D. Chowdhury, Phys. Rev. B **95**, 060201 (2017), arXiv:1608.03280 [cond-mat.str-el].
- [5] K. Hashimoto, K. Murata, and R. Yoshii, Journal of High Energy Physics **10**, 138 (2017), arXiv:1703.09435 [hep-th].
- [6] M. Grttner, J. Bohnet, A. Safavi-Naini, M. L. Wall, J. J. Bollinger, and A. Rey, Nature Physics, **13** (2016).
- [7] X. Chen, T. Zhou, D. A. Huse, and E. Fradkin, Annalen der Physik **529**, 1600332.
- [8] Y. Sekino and L. Susskind, Journal of High Energy Physics **2008**, 065 (2008).
- [9] J. Maldacena, S. H. Shenker, and D. Stanford, Journal of High Energy Physics **2016**, 106 (2016).
- [10] M. Heyl, F. Pollmann, and B. Dóra, Phys. Rev. Lett. **121**, 016801 (2018).
- [11] M. Srednicki, Journal of Physics A Mathematical General **32**, 1163 (1999), cond-mat/9809360.
- [12] M. Srednicki, in *eprint arXiv:chao-dyn/9511001* (1995).
- [13] D. J. Luitz and Y. Bar Lev, Phys. Rev. B **96**, 020406 (2017).
- [14] S. Popescu, A. J. Short, and A. Winter, Nature Physics **2**, 754 (2006).
- [15] B. Swingle, G. Bentsen, M. Schleier-Smith, and P. Hayden, Phys. Rev. A **94**, 040302 (2016).
- [16] C. B. Dağ and L.-M. Duan, ArXiv e-prints (2018), arXiv:1807.11085 [quant-ph].
- [17] M. Rigol, V. Dunjko, and M. Olshanii, Nature (London) **452**, 854 (2008), arXiv:0708.1324 [cond-mat.stat-mech].
- [18] C. B. Dağ, S.-T. Wang, and L.-M. Duan, Phys. Rev. A **97**, 023603 (2018).
- [19] Q. Wang and F. Pérez-Bernal, arXiv e-prints , arXiv:1812.01920 (2018), arXiv:1812.01920 [quant-ph].
- [20] Z.-H. Sun, J.-Q. Cai, Q.-C. Tang, Y. Hu, and H. Fan, arXiv e-prints , arXiv:1811.11191 (2018), arXiv:1811.11191 [quant-ph].
- [21] F. Franchini, ed., *Lecture Notes in Physics, Berlin Springer Verlag*, Lecture Notes in Physics, Berlin Springer Verlag, Vol. 940 (2017) arXiv:1609.02100 [cond-mat.stat-mech].
- [22] V. L. Berezinskiĭ, Soviet Journal of Experimental and Theoretical Physics **32**, 493 (1971).
- [23] J. M. Kosterlitz and D. J. Thouless, Journal of Physics C Solid State Physics **5**, L124 (1972).

Supplementary: Detection of quantum phases via out-of-time-order correlators

EFFECT OF FLUCTUATIONS

Here we give the additional results of XXZ model on the relation between OTOCs and phase transitions. Fig. S1 shows the difference between the OTOC saturation values (already depicted in the main text as Fig. 1) and the ground state contribution in these values. The mismatch between OTOC saturation value and ground state contribution to it is clear in XY-phase, due to the fact that the correction term of the excitations is dominant in the XY-phase, as explained in the text.

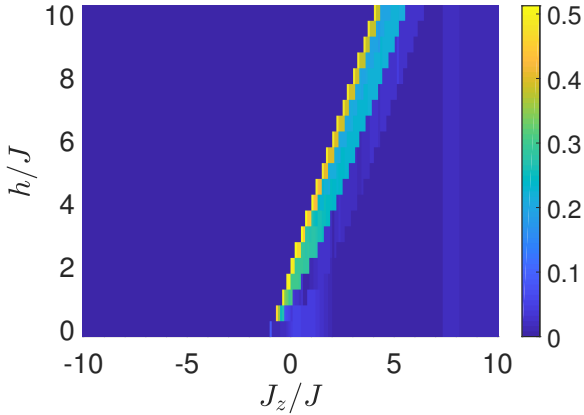


FIG. S1. The difference between the OTOC saturation values (via Eq. (4) in main text) and the ground state contribution for the phase diagram while the x-axis is the spin interaction strength in the z-direction J_z and y-axis is the magnetic field h , for $N = 13$ system size and σ_z^i where the observation spin is chosen from bulk, when open boundary conditions are set and the initial state is a ground state.

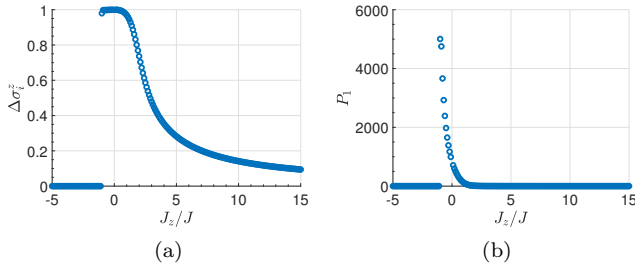


FIG. S2. (a) Fluctuations in the operator σ_z^i of a bulk spin with respect to the ground state of the corresponding phase for a system size $N = 15$. (b) Participation ratio of the ground state with respect to J_z/J for a system size $N = 15$, while the reference basis is spin basis.

Fig. S2b shows the fluctuations, $(\Delta\sigma_z^i)^2 = \langle(\sigma_z^i)^2\rangle -$

$\langle\sigma_z^i\rangle^2$ while the expectation value is over the ground state ψ_1 . Fig. S2 shows the participation ratio (PR) value of the ground state in terms of spin basis. PR is defined as

$$P_\alpha = \left(\sum_{n=1} |\psi_{\alpha n}|^4 \right)^{-1}, \quad (\text{S1})$$

where α are eigenstates and n are the reference basis. PR is a measure of fluctuations of a state in a reference basis. We see that the ferromagnetic ground states ($J_z/J < -1$) are more localized compared to anti-ferromagnetic ground states ($J_z/J > 1$), because of the subspaces that they belong to under a S_z conserving Hamiltonian. As a result, anti-ferromagnetic ground states are more susceptible to both finite-size effects (mixing in energy levels) and the effect of the rest of the terms in the Hamiltonian. This is also the reason why OTOCs are better in capturing the transition from a ferromagnet to a XY-paramagnet compared to anti-ferromagnet to XY-paramagnet. We see that the PR values for XY-phase are the maximum, even though they are around the half of the size of subspace $S_z = \pm 1$ in odd-numbered chains and $S_z = 0$ in even-numbered chains. The fluctuations in σ_z^i operator are exactly zero in the ferromagnetic region, as mentioned in the main text and seen in Fig. S2b, whereas they are approximately zero in anti-ferromagnetic region. Unless $J_z \gg J$, the XX- and YY-coupling terms cause the Neel states to slightly couple to the other states in $S_z = 0$ subspace. The fluctuations are maximized in XY-phase, causing a dominant correction term. We finally note that the fluctuations are always maximum for the quasi-long range operator σ_x^i .

EFFECT OF FINITE-SIZE AND DIFFERENT BOUNDARY CONDITIONS

In this section, we show how choosing a finer resolution in energy levels and hence studying the long-time dynamics might affect the results severely due to finite-size. Due to the level mixing in the degenerate ground states of even-numbered chains, finite-size gap opening is more severe in the transition from XY- to anti-ferromagnetic phase for even-numbered chains. In the main text, we restrict the effect of finite-size via choosing an experimentally more realistic time scale, and effectively choosing a coarse resolution in the energy level structure. In Fig. S3 we show how the finite-size effect could plague the OTOC in the detection of anti-ferromagnetic order when we choose long enough times to simulate $t < \frac{\pi}{4} 10^3 [1/J]$. This is a good example of how finite-size effects could turn the scrambling into a pre-scrambling effect, restricting the order to short-times. Fig. S4 is the phase diagram of even-numbered chains with phase boundaries dictated by the Bethe ansatz for an infinite-size chain.

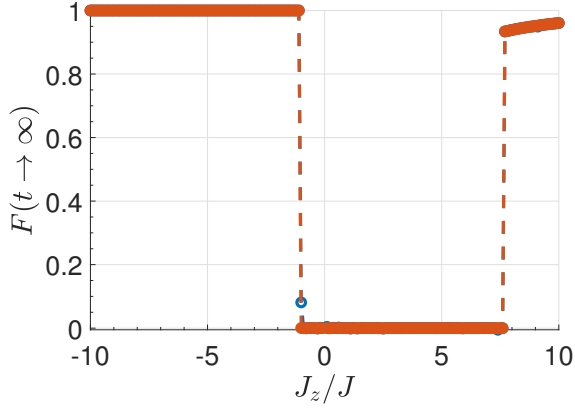


FIG. S3. OTOC saturation value (Eq. (4), blue line) and its ground state contribution (Eq. (6), orange line) for $h = 0$ [J], $N = 14$ and for time $t \lesssim \frac{\pi}{4} 10^3$ [1/J]. The anti-ferromagnetic order is concealed due to finite-size effects appearing in long-times.

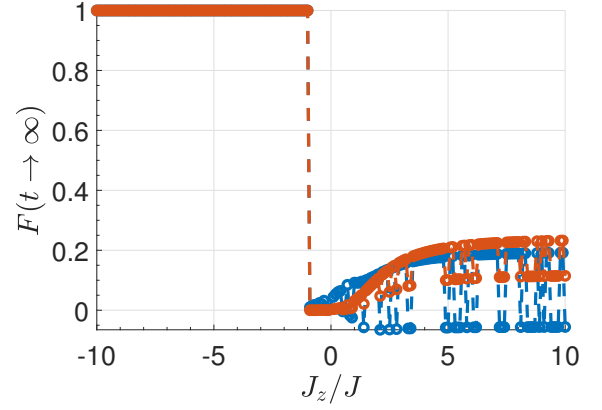


FIG. S6. OTOC saturation value (Eq. (4), blue line) and its ground state contribution (Eq. (6), orange line) for $h = 0$ [J] when $N = 13$ is set and for time $t \lesssim \frac{\pi}{4} 10^3$ [1/J] with periodic boundary conditions.

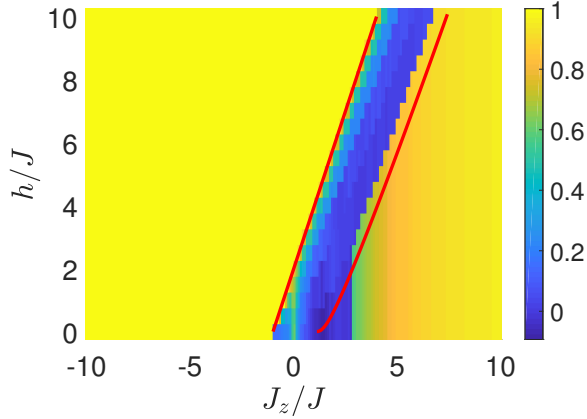


FIG. S4. The OTOC phase diagram (via Eq. (4)) for even-numbered chains while the x-axis is the spin interaction strength in the z-direction J_z [J] and y-axis is the magnetic field h [J], for $N = 14$ system size and σ_z^i where the observation spin is chosen from bulk, when periodic boundary conditions are set and initial state is a ground state. The time-scale where the results are valid is $\frac{\pi}{4} 10^1$ [1/J].

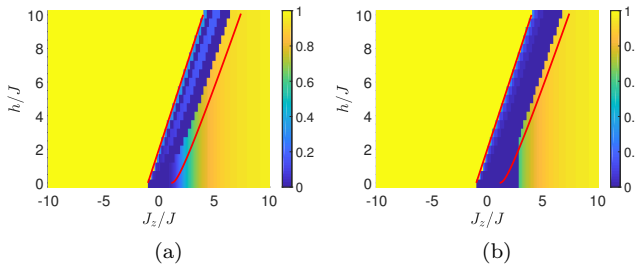


FIG. S5. Ground state value contribution (Eq. (6)) to OTOC for (a) odd-numbered $N = 13$ and (b) even-numbered $N = 14$ chains.

The finite-size effects for small fields are more severe than odd-numbered chains, but approaches to similar results as the magnetic field h increases. The difference between Bethe ansatz results and the OTOC phase boundary for the anti-ferromagnetic to XY phase in high fields is also due to finite-size effects. This could be seen in Figs. S5, where we compare the ground state value in OTOC with the exact phase boundaries. Same difference for anti-ferromagnetic to XY phase boundary can be seen too. This points to the effect of finite-size rather than the incapability of OTOC to probe the phase transition as precisely as exact results.

Finally we present the result for odd-numbered chain if periodic boundary condition is applied, Fig. S6. The low values and fluctuations in the anti-ferromagnetic region are a sign of how OTOC is sensitive to emerging domain walls in the ground state.